Chiang Mai J. Sci. 2018; 45(4) : 1921-1932
http://epg.science.cmu.ac.th/ejournal/
Contributed Paper

Stable and Metastable Phase Equilibria in the Ternary System MgB_4O_7-$MgSO_4$-H_2O at 273 K

Tingting Zhang [a], Wenyao Zhang [a], Ruizhi Cui [b], Yunyun Gao [b] and Shihua Sang* [a]

[a] College of Materials and Chemistry & Chemical Engineering, Chengdu University of Technology, Chengdu 610059, P. R. China.

[b] Mineral Resources Chemistry Key Laboratory of Sichuan Higher Education Institutions, Chengdu 610059, P. R. China.

* Author for correspondence; e-mail: sangshihua@sina.com.cn

Received: 19 September 2016
Accepted: 1 March 2017

ABSTRACT

The stable and metastable phase equilibria of the ternary system $MgSO_4$-MgB_4O_7-H_2O at 273 K were measured respectively using isothermal solubility equilibrium method and isothermal evaporation crystallization method. The solubilities and densities of equilibrium liquid phase in the system were determined. Based on the experimental data and the corresponding equilibrium solid phase, the stable and metastable phase diagrams and their corresponding density versus composition diagrams in this system were plotted, respectively. A comparative analysis of the stable and metastable phase diagrams were made, in addition to, compared with stable phase diagrams at 273 K and 298 K in the system. Experimental results show that both the stable and metastable phase diagrams are constituted by a eutectic point for ($MgSO_4 \cdot 7H_2O$+$MgB_4O_7 \cdot 9H_2O$), two univariant solubility curves, two solid phase crystalline regions corresponding to $MgSO_4 \cdot 7H_2O$ and $MgB_4O_7 \cdot 9H_2O$. Compared with the stable phase diagram, the sizes of the crystalline regions are different in the metastable phase diagram. Both the stable and metastable phase equilibria in the system at 273 K are simple cosaturated type and there are no complex salt or solid solution were found.

Keywords: stable equilibrium, metastable equilibrium, solubility, $MgSO_4$, MgB_4O_7

1. INTRODUCTION

A large of brine resources were discovered, in Qinghai, China. The resources are extensively used in high-efficiency agriculture, information technology, energy, non-ferrous materials, environmental protection and other industries [1]. Qaidam Basin salt lakes are a subtype of magnesium sulfate brines, which are famous for abundant salt lakes with high concentrations of lithium, potassium, magnesium, and boron resources. The brines mostly belong to the complex seven-component system of Li^+, Na^+, K^+, Mg^{2+}//Cl^-, SO_4^{2-}, borate-H_2O [2].

In order to economically exploit the brine and mineral resources, it is of great importance to research the phase diagrams for salt lakes. As a part of the complex system, stable phase diagrams of some four-or

five-component subsystems have been measured. [3-8]. However, salt lakes are naturally formed complex multicomponent systems under water and salt interaction. For studying on phase equilibria, it is not enough to only study stable phase equilibria in the natural evaporation crystallization process of salt lake brine. Because there are the phenomena of supersaturation of the brines found in salt lakes. For example, some containing sulfate and borate systems [9-12] were reported. Therefore, metastable phase equilibria research is essential to predict the crystallized path of evaporation of the salt lake brine.

Although the industry program always proceed at room temperature, the design of the complete process route is inseparable from the theoretical guidance of the multi-temperature water and salt system phase diagrams. Therefore, it is imperative to study the phase equilibrium of water and salt system at different temperatures. Importantly, Qaidam Basin have a typical climate conditions, are generally windy, arid, little rainfall, and great evaporating capacity. In recent years, based on this climate, Zeng and Sang [13-18] have studied some metastable equilibria containing lithium, sodium, potassium, and boron at 273 K. Recently, the complex system Li^+, K^+, Mg^{2+} //Cl^-, SO_4^{2-}, $B_4O_7^{2-}$-H_2O and its subsystem at 273 K were studied successively by our group. As a subsystem, the stable and metastable phase equilibria of the ternary system $MgSO_4$-MgB_4O_7-H_2O at 273 K were measured in this paper, respectively. More significantly, a comparison of the stable and metastable phase equilibria is to predict accurately the crystallized path. Therefore, this study provides ternary system solubility data for the subsystem of complex system Li^+, K^+, Mg^{2+}//Cl^-, SO_4^{2-}, $B_4O_7^{2-}$-H_2O, and some reference value for industrial development of inorganic saltsin salt lake.

2. MATERIALS AND METHODS

2.1 Reagents and Instruments

The water was doubly deionized for the experimental samples preparation and quantitative analysis. It has an electrical conductivity less than 1×10^{-5} S·m^{-1} and pH≈6.60 at 298 K. The inorganic chemicals ($MgSO_4$ and other auxiliary reagents) used in this work were all analytical purity grade and provided by Chengdu Kelong Chemical Reagent Manufactory, China, tabulated in Table 1. $MgB_4O_7 \cdot 9H_2O$ was synthesized by experimental methods in laboratory.

Table 1. Chemical sample descriptions.

Chemical name	Source	Initial Mole Fraction Purity	Purification Method	Final Mole Fraction Purity	Analysis Method
$MgSO_4$	Chengdu Kelong Chemical Reagent Manufactory	0.99	None	0.99	titration
MgO	Chengdu Kelong Chemical Reagent Manufactory	0.98	None	0.98	-
H_3BO_3	Chengdu Kelong Chemical Reagent Manufactory	0.995	None	0.995	-
$MgB_4O_7 \cdot 9H_2O$	Synthesis	-	chemical reaction	0.99	titration

A UPT-II-20T type Ultra-pure water (supplied by SichuanYoupu Instrument co., LTD) was applied to provide the deionized water. An AL104 type analytical balance of a 110 g capacity and 0.0001 g resolution (provided by the Mettler Toledo Instruments Co., Ltd.) was applied to determine the weight of samples. A SHH-250 type biochemical incubator of temperature range at 258~333 K and ±0.1 K resolution (supplied by the Chongqing Inborn Experiment Instrument co., LTD.) was employed to achieve the temperature. A HY-5 type cyclotron oscillator (supplied by the Jintan Kexi Instrument co., LTD) was applied to sample oscillation. An X-ray diffraction analyzer (DX-2700 with Cu Kα radiation) was used to analyze the phase composition of solid salt. The polyethylene containers (Length: 20 cm, width: 14 cm and height: 8 cm) were applied to metastable evaporation experiment.

2.2 Experimental Methods

The stable phase equilibria were studied using isothermal solubility equilibrium method [19]. The system points of the ternary systems were prepared by adding the other salt gradually on the basis of the binary invariant points at 273 K. Each sample was added doubly deionized water quantitatively for dissolving the prepared salts and loaded into clean sealed glass bottles. However, it must ensure the solid phases were not dissolved entirely in the whole experiment process. Then, the glass bottles were placed in the cyclotron oscillator (HY-5), which was put into the incubator (SHH-250) to controlled the internal temperature to 273 ± 0.1 K. The oscillator should be shook vigorously in order to sufficiently dissolve the salts. The supernatant of samples were taken out periodically for chemical analysis (Samples should be stationary at a constant temperature, so that the salt could sink completely). When the compositions of solution remain unchanged, the system has reached the thermodynamic equilibrium state. After equilibrium, we took out the liquid and solid phases separately. Then the liquid compositions were measured quantitatively by chemical methods, and the solid phases were determined by powder X-ray diffraction. The results show that it takes about 40 days for the ternary system to reach phase equilibrium.

The metastable phase equilibria were studied using isothermal evaporation crystallization method [19]. An appropriate quantity of salts and DDW were mixed together to produce a series of artificial synthesized brines. When the salts completely dissolved, the synthesized brines were placed in the open and clean polyethylene containers, which had been put into the biochemical incubator (SHH-250) beforehand. The experiment was carried out in the conditions of the internal temperature (273±0.1) K, wind velocity (4.0 to 4.4) $m \cdot s^{-1}$, a relative humidity (30 to 35) %. Throughout the course of the experiment, the artificial synthesized brines had been still left unstirred, and the crystal behaviors of the solid phase were observed periodically. When the new solid phases appeared in the polyethylene containers, the 5.00 mL supernatant was taken out with a pipette gun and then diluted to 100 mL in a volumetric flask, which was analyzed by chemical methods to obtain the compositions of salts. At the same time, the wet residue mixtures were removed from the solution and determined by powder X-ray diffraction. However, the remainder of the solution continued to be evaporated and reached a new metastable equilibrium point.

The densities of saturated solution were determined by pycnometer method both in

the stable and metastable phase equilibria of the aqueous ternary system. The specific method is that the 5.00 mL supernatant were taken out with a pipette gun quickly, then, weighed it as fast as possible.

2.3 Analytical Methods

The concentration of Mg^{2+} was evaluated using the EDTA complex titration method when the eriochrome black-T as an indicator, with a precision ±0.5% [20]. The concentration of borate ion ($B_4O_7^{2-}$) was measured through alkaline neutralization titration with the standard solution of NaOH (C=0.01 mol·L^{-1}), the phenolphthalein solution as an indicator when the mannitol existed, with an uncertainty of mass fraction within ±0.3% [21]. The concentration of SO_4^{2-} in liquid phase was analyzed by ion balance combined with gravimetric methods in the presence of barium chloride, with an uncertainty of mass fraction within ±0.5% [22]. The densities were measured with a density bottle method with an uncertainty of 0.0002 g·cm^{-3}. The equilibrium solid phases were analyzed by the X-ray diffractometer.

3. RESULTS AND DISCUSSIONS

3.1 Synthesis of $MgB_4O_7·9H_2O$

The $MgB_4O_7·9H_2O$ is one of equilibrium solid phases in ternary system MgO-B_2O_3-H_2O at 298 K. According to the new method of synthesis $MgB_4O_7·9H_2O$ provided by Jing [23], the purity is more than 99.0%, which can satisfy the need of the experiment study. We learned that the hungtsaoite ($MgB_4O_7·9H_2O$) was prepared by the materials of MgO and H_3BO_3, the mass ratio of MgO, H_3BO_3 and H_2O is 1:8:66. Then, the mixed solution was stirred with an agitator, which was placed in the thermostatic water bath at 298 K, the solution keep stirred until the turbid solution had clarified. Then, it had kept stirring after removed the insoluble. Finally, a mass of white precipitate was found. It takes about three days to obtain the $MgB_4O_7·9H_2O$. The X-ray diffraction pattern of the hungtsaoite ($MgB_4O_7·9H_2O$) is shown in Figure 1.

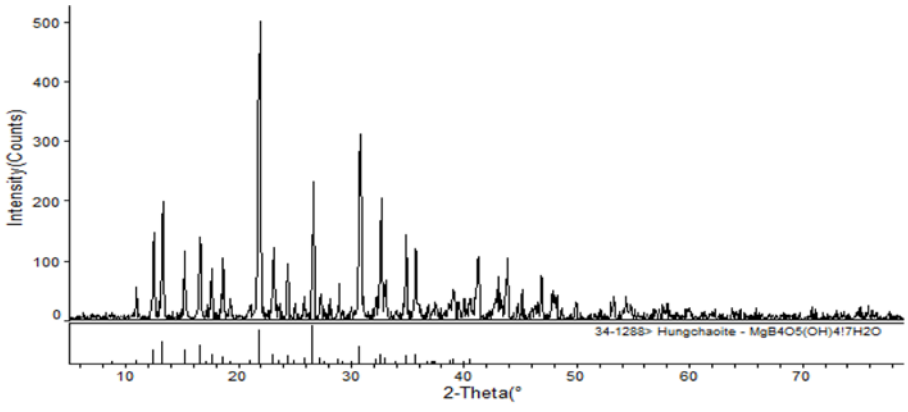

Figure 1. X-ray diffraction pattern of the Hungtsaoite [$MgB_4O_7·9H_2O$].

3.2 The Stable Phase Equilibria of MgB_4O_7-$MgSO_4$-H_2O at 273 K

After chemical analysis, the solubilities of the salt and densities of equilibrium solution in this system are listed in Table 2. The mass fraction of salt B is noted as w (B), and the density of solution is noted as ρ/g·cm^{-3}. The stable phase diagram of ternary system MgB_4O_7-$MgSO_4$-H_2O is plotted in Figure 2. On the basis of the experimental data, Figure 3 is the partial enlarged diagram. The density composition diagram is presented in Figure 4, the crystallization forms of the invariant point E_1(MgB_4O_7·$9H_2O$+$MgSO_4$·$7H_2O$) solid phase were determined with an X-ray diffraction analysis method and demonstrated in Figure 5.

Table 2. Solubilities and densities of the stable phase equilibrium for ternary system MgB_4O_7-$MgSO_4$-H_2O at 273 K.

No	Composition of solution/%		Density	Solid
	100·w($MgSO_4$)	100·w(MgB_4O_7)	ρ/g·cm^{-3}	phase
1, A_1	0.00	0.45	1.013	MgB_4O_7·$9H_2O$
2	2.25	0.46	1.032	MgB_4O_7·$9H_2O$
3	4.98	0.52	1.059	MgB_4O_7·$9H_2O$
4	5.94	0.53	1.068	MgB_4O_7·$9H_2O$
5	9.59	0.54	1.104	MgB_4O_7·$9H_2O$
6	12.87	0.55	1.139	MgB_4O_7·$9H_2O$
7	15.91	0.56	1.170	MgB_4O_7·$9H_2O$
8	17.90	0.57	1.192	MgB_4O_7·$9H_2O$
9	18.90	0.58	1.203	MgB_4O_7·$9H_2O$
10	19.71	0.59	1.212	MgB_4O_7·$9H_2O$
11	20.45	0.62	1.222	MgB_4O_7·$9H_2O$
12,E_1	20.88	0.65	1.228	MgB_4O_7·$9H_2O$+$MgSO_4$·$7H_2O$
13	20.90	0.57	1.226	$MgSO_4$·$7H_2O$
14	21.14	0.40	1.223	$MgSO_4$·$7H_2O$
15	21.15	0.33	1.222	$MgSO_4$·$7H_2O$
16	21.17	0.27	1.222	$MgSO_4$·$7H_2O$
17	21.21	0.25	1.221	$MgSO_4$·$7H_2O$
18	21.23	0.18	1.221	$MgSO_4$·$7H_2O$
29	21.27	0.14	1.217	$MgSO_4$·$7H_2O$
20, B_1	21.08	0.00	1.200	$MgSO_4$·$7H_2O$

[a] Standard uncertainties u are u(T) = 0.50 K; u_r (p) =0.9 KPa.; u_r (ρ) = 2.0·10^{-4} g/cm^{-3}; u_r (MgB_4O_7) = 0.0050; u_r ($MgSO_4$) = 0.0020; w(B), mass fraction of B;

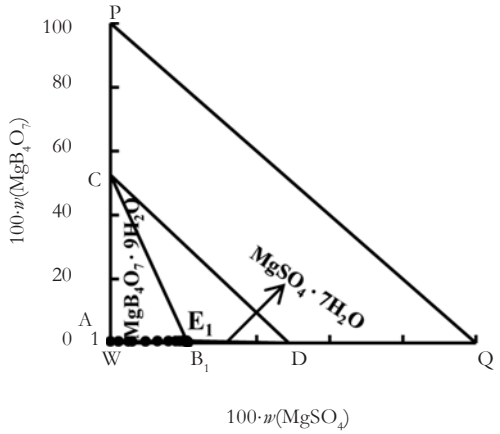

Figure 2. Stable phase diagram of ternary system MgB_4O_7-$MgSO_4$-H_2O at 273 K.

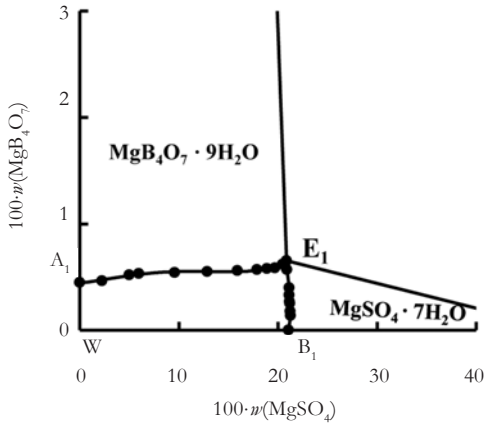

Figure 3. Partial enlarged diagram of Figure 2.

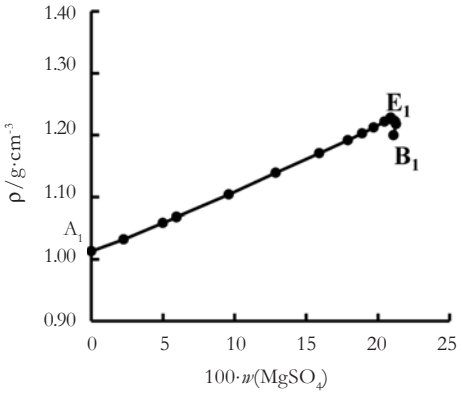

Figure 4. Density composition diagram of the stable phase equilibrium for ternary system MgB_4O_7-$MgSO_4$-H_2O at 273 K.

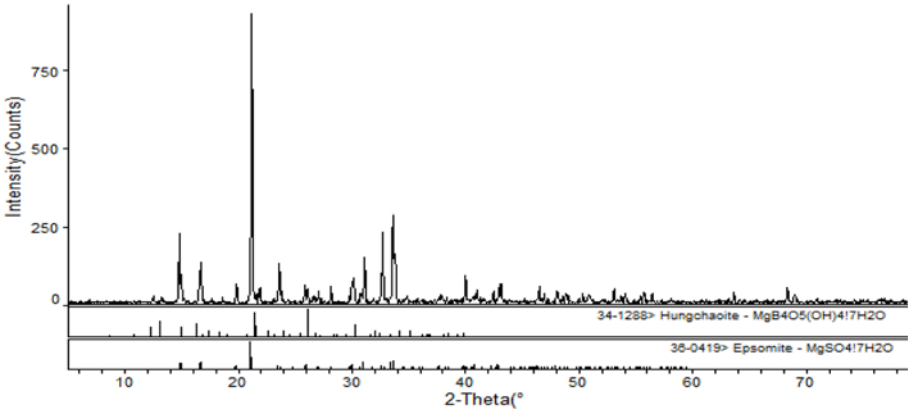

Figure 5. X-ray diffraction pattern of the eutectic point E_1 [$MgB_4O_7 \cdot 9H_2O$ + $MgSO_4 \cdot 7H_2O$] in the stable phase equilibrium for ternary system MgB_4O_7-$MgSO_4$-H_2O at 273 K.

According to the Table 2, Figures 2 and 3, the stable phase diagram consists of one invariant point E_1, which is saturated with salts $MgB_4O_7{\cdot}9H_2O$ and $MgSO_4{\cdot}7H_2O$. The composition of the equilibrium solution is $w(MgB_4O_7)$=0.65% and $w(MgSO_4)$=20.88%. There are two univariant solubility curves (A_1E_1, B_1E_1), and two solid crystalline phase regions (A_1E_1C, B_1E_1D), which corresponding to two single salts, hungchaoite ($MgB_4O_7{\cdot}9H_2O$) and epsomite ($MgSO_4{\cdot}7H_2O$), respectively. It is significant difference that the solid crystalline phase regions (A_1E_1C) of $MgB_4O_7{\cdot}9H_2O$ is larger than the (B_1E_1D) of $MgSO_4{\cdot}7H_2O$ in the phase diagram, which means that the salt $MgB_4O_7{\cdot}9H_2O$ has smaller solubility among the coexisting salts. The area (CE_1D) is the common crystallization area of $MgB_4O_7{\cdot}9H_2O$ and $MgSO_4{\cdot}7H_2O$, and the area ($WA_1E_1B_1W$) is unsaturated single liquid region. It is found that there are neither complex salt nor solid solution formed. Therefore, it belongs to a simple eutectic type.

From Table 2 and Figure 4, it is seen that the solubility of magnesium sulfate is much greater than that of magnesium borate among the coexisting salts at 273 K. Thus, the density is mainly affected by the magnesium sulfate content in the equilibrium solution. On account of this, the densities versus composition is plotted according to the $w(MgSO_4)$. It is found that the densities of solution increase with the increasing of $w(MgSO_4)$, at the invariant point E_1, the density becomes the largest one.

The stable phase equilibrium of ternary system MgB_4O_7-$MgSO_4$-H_2O at 298 K had been reported by Song [24]. A part of the experiment data for the ternary system at 273 K and 298 K are listed in Table 3. On the basis of the data, the phase diagrams are plotted in Figure 6. From Figure 6, it can be seen that the crystallization forms of the salts are not changed with the increase of temperature, are $MgB_4O_7{\cdot}9H_2O$ and $MgSO_4{\cdot}7H_2O$, whereas the crystallization zones of salts have changed, the crystallization zone of $MgB_4O_7{\cdot}9H_2O$ obviously increased at 298 K. From Table 3, the solubilities of MgB_4O_7 and $MgSO_4$ obviously increase with increasing of temperature from 273 K to 298 K. The mass fractions composition of the corresponding liquid phase at 273 K are $w(MgB_4O_7)$=0.45%, $w(MgSO_4)$=21.08%, are $w(MgB_4O_7)$=0.64% and w($MgSO_4$)=26.78% at 298 K. The liquid compositions also significantly increase at the eutectic point, the mass fractions are $w(MgB_4O_7)$=0.65%, $w(MgSO_4)$=20.88% at 273 K, are $w(MgB_4O_7)$=1.02% and $w(MgSO_4)$=26.54% at 298 K, respectively. Therefore, the decrease of temperature is beneficial to the crystallization of magnesium borate.

Table 3. Solubilities of saturated solution in the stable phase equilibrium for ternary system MgB_4O_7-$MgSO_4$-H_2O at 273 K and 298 K [24].

Temperature	Composition of solution/%		Systems	Solid phase
	$100{\cdot}w(MgSO_4)$	$100{\cdot}w(MgB_4O_7)$		
237 K	21.08	0	$MgSO_4$-H_2O	$MgSO_4{\cdot}7H_2O$
	20.88	0.65	MgB_4O_7-$MgSO_4$-H_2O	$MgB_4O_7{\cdot}9H_2O$+ $MgSO_4{\cdot}7H_2O$
	0	0.45	MgB_4O_7-H_2O	$MgB_4O_7{\cdot}9H_2O$
298 K [24]	26.78	0	$MgSO_4$-H_2O	$MgSO_4{\cdot}7H_2O$
	26.54	1.02	MgB_4O_7-$MgSO_4$-H_2O	$MgB_4O_7{\cdot}9H_2O$+ $MgSO_4{\cdot}7H_2O$
	0	0.64	MgB_4O_7-H_2O	$MgB_4O_7{\cdot}9H_2O$

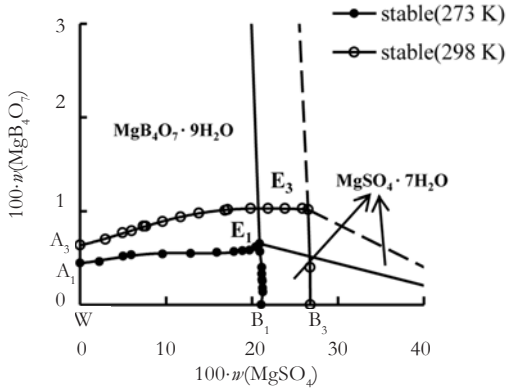

Figure 6. Sable phase diagrams of ternary system MgB_4O_7-$MgSO_4$-H_2O at 273 K and 298 K [24].

3.3 The Metastable phase equilibria of MgB_4O_7-$MgSO_4$-H_2O at 273 K

Similarly, the solubilities and densities of the metastable phase equilibrium for the ternary system MgB_4O_7-$MgSO_4$-H_2O are listed Table 4. According to the experimental data, the metastable phase diagram is shown in Figure 7, and Figure 8 is the partial enlarged diagram. The density composition diagram is presented in Figure 9, the X-ray diffraction pattern of the invariant point E_2 ($MgB_4O_7 \cdot 9H_2O$+$MgSO_4 \cdot 7H_2O$) is given in Figure 10.

Table 4. Solubilities and densities in the metastable phase equilibrium for ternary system MgB_4O_7-$MgSO_4$-H_2O at 273 K.

No	Compositionof solution/%		Density	Solid
	$100 \cdot w(MgSO_4)$	$100 \cdot w(MgB_4O_7)$	ρ/g·cm^{-3}	phase
1,A_2	0.00	0.53	1.018	$MgB_4O_7 \cdot 9H_2O$
2	3.92	0.58	1.059	$MgB_4O_7 \cdot 9H_2O$
3	4.67	0.62	1.068	$MgB_4O_7 \cdot 9H_2O$
4	5.70	0.65	1.080	$MgB_4O_7 \cdot 9H_2O$
5	7.07	0.69	1.095	$MgB_4O_7 \cdot 9H_2O$
6	9.77	0.70	1.123	$MgB_4O_7 \cdot 9H_2O$
7	11.80	0.72	1.146	$MgB_4O_7 \cdot 9H_2O$
8	14.93	0.78	1.178	$MgB_4O_7 \cdot 9H_2O$
9	18.58	0.84	1.210	$MgB_4O_7 \cdot 9H_2O$
10	19.38	0.90	1.219	$MgB_4O_7 \cdot 9H_2O$
11	19.98	0.99	1.224	$MgB_4O_7 \cdot 9H_2O$
12,E_2	20.45	1.03	1.231	$MgB_4O_7 \cdot 9H_2O$+$MgSO_4 \cdot 7H_2O$
13	20.44	1.02	1.230	$MgSO_4 \cdot 7H_2O$
14	20.48	0.91	1.229	$MgSO_4 \cdot 7H_2O$
15	20.59	0.87	1.228	$MgSO_4 \cdot 7H_2O$
16	20.74	0.76	1.226	$MgSO_4 \cdot 7H_2O$
17	20.87	0.67	1.226	$MgSO_4 \cdot 7H_2O$
18	20.92	0.50	1.223	$MgSO_4 \cdot 7H_2O$
19	21.19	0.28	1.221	$MgSO_4 \cdot 7H_2O$
20	21.44	0.14	1.218	$MgSO_4 \cdot 7H_2O$
21,B_2	21.70	0.00	1.209	$MgSO_4 \cdot 7H_2O$

[a] Standard uncertainties u are u(T) = 0.50 K; u_r (p) =0.9 KPa.; u_r (ρ) = $2.0 \cdot 10^{-4}$ g/cm^{-3}; u_r (MgB_4O_7) = 0.0050; u_r ($MgSO_4$) = 0.0020; w(B), mass fraction of B;

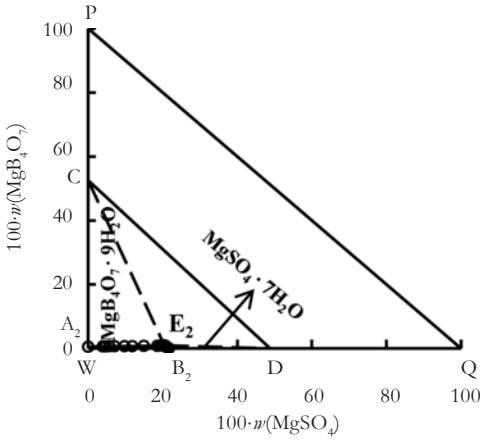

Figure 7. Metastable phase diagram in the ternary system MgB_4O_7-$MgSO_4$-H_2O at 273 K.

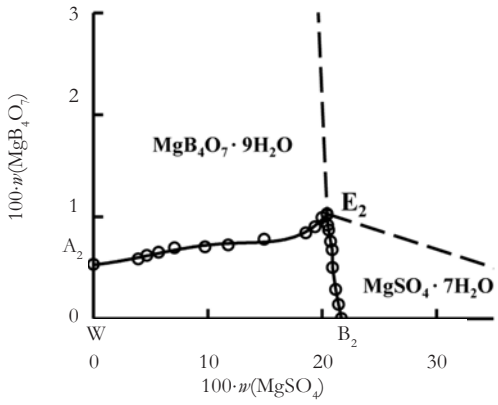

Figure 8. Partial enlarged diagram of the Figure 7.

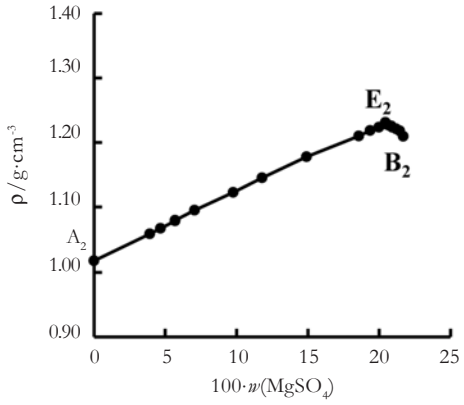

Figure 9. Density composition diagram of the metastable phase equilibrium for ternary system MgB_4O_7-$MgSO_4$-H_2O at 273 K.

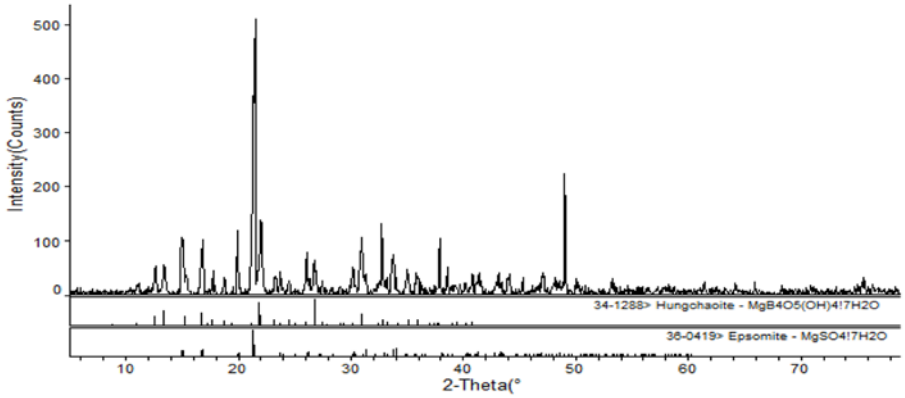

Figure 10. X-ray diffraction pattern of the eutectic point E_2 [$MgB_4O_7 \cdot 9H_2O$ + $MgSO_4 \cdot 7H_2O$] in the metastable phase equilibrium for ternary system MgB_4O_7-$MgSO_4$-H_2O at 273 K.

It is a focus to compare the stable with metastable phase equilibrium for the ternary system MgB_4O_7-$MgSO_4$-H_2O at 273 K in this paper. A comparison chart of the stable and metastable phase diagrams is presented in Figure 11.

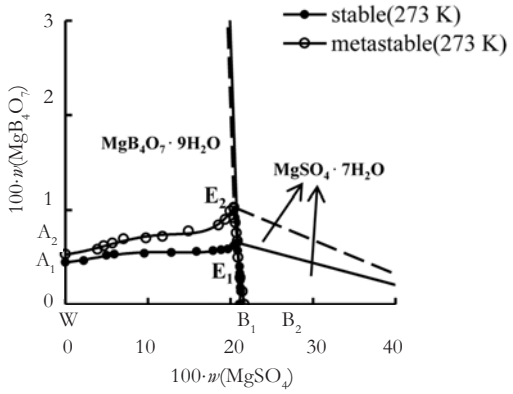

Figure 11. Comparison chart in the stable and metastable phase diagrams.

There are some similarities in the stable and metastable phase equilibrium for the ternary system MgB_4O_7-$MgSO_4$-H_2O at 273 K. From Tables 2 and 4, and Figure 11, it is found that the metstable phase diagram belongs to a simple co-saturation type, there are neither solid solutions nor double salts are formed. The reason may be that the lattice type, lattice parameters, and atomic structure of $MgB_4O_7 \cdot 9H_2O$ and $MgSO_4 \cdot 7H_2O$ are quite different. The $MgSO_4 \cdot 7H_2O$ is a columnar crystal, but the $MgB_4O_7 \cdot 9H_2O$ is a powdery crystal. Therefore, it is difficult to form double salts and solid solution between the two salts. Analogously, it consists of one invariant point E_2 is comprised by $MgB_4O_7 \cdot 9H_2O$ and $MgSO_4 \cdot 7H_2O$, two univariant isothermal metastable solubility curves (A_2E_2, B_2E_2). Two solid phase crystallization zones (A_2E_2C, B_2E_2D) corresponding to $MgB_4O_7 \cdot 9H_2O$ and $MgSO_4 \cdot 7H_2O$, respectively. The area (CE_2D) is the common crystallization area of $MgB_4O_7 \cdot 9H_2O$ and $MgSO_4 \cdot 7H_2O$, and the area ($WA_2E_2B_2W$) is unsaturated single liquid region. From the Figure 9, the relationship between density and composition of magnesium sulfate in the metstable ternary system MgB_4O_7-$MgSO_4H_2O$ at 273 K. It is found that the densities are gradually increased regularly with increasing the magnesium sulfate concentration in the solution, and becomes the largest one at the invariant point E_2.

However, there are many differences between the stable phase equilibrium and metastable phase equilibrium. The single salts ($MgB_4O_7 \cdot 9H_2O$ and $MgSO_4 \cdot 7H_2O$) solubilities in the metastable phase diagram are greater than that the stable phase diagram. The mass fractions of single salts are $w(MgB_4O_7)$=0.53%, $w(MgSO_4)$=21.70% in the metastable phase diagram, however, they are corresponding to $w(MgB_4O_7)$=0.45%, $w(MgSO_4)$= 21.08% in the stable phase diagram. In the eutectic point, the mass fractions of liquid phase are $w(MgB_4O_7)$= 1.03%, w(MgSO4)=20.45% in the metastable phase diagram. But, the mass fractions are $w(MgB_4O_7)$=0.65%, $w(MgSO_4)$= 20.88% in the stable phase diagram. It can be seen that the solubility of MgB_4O_7 in the metastable phase diagram are obviously increased than that the stable phase diagram, which illustrates that there some supersaturated phenomena for MgB_4O_7 at 273 K in the metastable phase equilibrium. It may be due to the speed of the crystal formation, probably the speed of nucleation and the speed of grow up of crystal is very slow for MgB_4O_7 in the solution, so that the chemical potential of the salt (MgB_4O_7) in the liquid phase is greater than the solid phase in the process of evaporation[19].

4. CONCLUSIONS

The stable and metastable phase equilibria for the ternary system MgB_4O_7-$MgSO_4$-H_2O

at 273 K were studied using isothermal solubility equilibrium method and isothermal evaporation crystallization method, respectively. Based on the experimental data, the stable and metastable phase diagrams and the density composition diagrams were drawn. The results show that both the stable and metastable phase diagrams belong to the simple co-saturation type. The solid phase crystalline region of $MgB_4O_7 \cdot 9H_2O$ is larger than $MgSO_4 \cdot 7H_2O$, so that the salt $MgB_4O_7 \cdot 9H_2O$ has smaller solubility among the coexisting salts. Besides, the densities composition show a regular variation, there are a maximum in the eutectic point both in the stable and metastable phase equilibria.

Compared with the stable phase diagram in the ternary system MgB_4O_7-$MgSO_4$-H_2O at 273 K, the crystalline region of $MgSO_4$ and MgB_4O_7 have changed, there is a supersaturated phenomenon for MgB_4O_7 in the metastable phase equilibrium.

Finally, the salts $MgSO_4$ and MgB_4O_7 have the same crystallization forms ($MgB_4O_7 \cdot 9H_2O$ and $MgSO_4 \cdot 7H_2O$) in stable and metastable phase equilibria for the aqueous ternary system MgB_4O_7-$MgSO_4$-H_2O at 273 K, including the stable phase equilibrium at 298 K. The solubilities of two salts in water increasing with the increase of temperature.

ACKNOWLEDGMENTS

This project was supported by the National Natural Science Foundation of China (U1407108), scientific research and innovation team in Universities of Sichuan Provincial Department of Education (15TD0009)

REFERENCES

[1] Zhou Y., Li L.J. and Wu Z.J., *J. Progress Chem.*, 2013; **25**: 1613-1624.

[2] Wang S.Q. and Deng T.L., *J. Chem. Thermodynamics*, 2008; **40**: 1007-1011. DOI 10.1016/j.jct.2008.02.008.

[3] Sun B., Song P.S. and Du X.H., *J. Salt Lake Sci.*, 1994; **2**: 26-30.

[4] Sang S.H. and Peng J., *Computer Coupling of Phase Diagrams and Thermochemistry*, 2010; **34**: 64-67. DOI 10.1016/j.calphad.2009.12.001.

[5] Sang S., Li M., Li H. and Sun M.L., *J. Acta Geologica Sinica*, 2010; **84**: 1704-1707.

[6] Zhou H.Y., Zeng Z.W., Han H.J., Dong O.Y., Li D.D. and Yao Y.J., *Chem. Eng. Data*, 2013; **58**: 1692-1696. DOI 10.1021/je4001125.

[7] Meng L.Z., Li D., Guo Y.F. and Deng T.L., *J. Chem. Eng. Data*, 2011; **56**: 5060-5065. DOI 10.1021/je2006852.

[8] Meng L.Z. and Deng T.L., *Russian J. Inorg. Chem.*, 2011; **56**: 1335-1338.

[9] Liu Y.H., Deng T.L. and Song P.S., *J. Chem. Eng. Data*, 2011; **56**: 1139-1147. DOI 10.1021/je1010888.

[10] Meng L.Z., Yu X.P., Li D. and Deng T.L., *J. Chem. Eng. Data*, 2011; **56**: 4627-4632. DOI 10.1021/je200563j.

[11] Deng T.L., Yu X. and Sun B., *J. Chem. Eng. Data*, 2008; **53**: 2496-2500. DOI 10.1021/je800245m.

[12] Deng T.L., Meng L.Z. and Sun B., *J. Chem. Eng. Data*, 2008; **53**: 704-709. DOI 10.1021/je700552j.

[13] Wang R.L. and Zeng Y., *J. Chem. Eng. Data*, 2014; **59**: 903-911. DOI 10.1021/je4010867.

[14] Zeng Y., Feng S. and Zheng Z.Y., *J. Chem. Eng. Data*, 2010; **55**: 5834-5838. DOI 10.1021/je100791a.

[15] Sang S.H., Lei N.F., Cui R.Z. and Qu S.D., *J. Chem. Eng. Chin. Univ.*, 2014; **28**: 21-26.

[16] Zeng Y., Cao F.J., Li L.G., Yu X.D. and Lin X.F., *J. Chem. Eng. Data*, 2011; **56**: 2569-2573. DOI 10.1021/je200091k.

[17] Peng Y., Zeng Y. and Su S., *J. Chem. Eng. Data*, 2011; **56**: 458-463. DOI 10.1021/je100843m.

[18] Zhang J.Q., Zeng Y., Peng Y. and Zong B., *J. Chem. Eng. Data*, 2013; **58**: 441-445. DOI 10.1021/je301160b.

[19] Niu Z.D. and Cheng F.Q., Tianjin University Press, Tianjin, 2002.

[20] Institute of Qinghai, *Salt-Lake of Chinese Academy of Sciences*, Chinese Science Press, Beijing, China, 1984.

[21] Fu C., Sang S.H., Zhou M.F., Liu Q.Z. and Zhang T.T., *J. Chem. Eng. Data*, 2016; **61**: 1071-1077. DOI 10.1021/acs.jced.5b00570.

[22] Deng T.L., Yin H.J. and Guo Y.F., *J. Chem. Eng. Data*, 2011; **56**: 3585-3588. DOI 10.1021/je200429a.

[23] Jing Y., Sea-Lake Salt & Chem. J. Ind., 2000; **29**: 24-25.

[24] Song P.S., Du X.H. and Sun B., *J. Chin. Sci. Bull.*, 1987; **19**: 1492-1495.